



# COMPARISON OF HEAT AND MASS TRANSFER PDE MODELS WITH TRADITIONAL ALGEBRAIC CORRELATIONS FOR ESTIMATING THE PERFORMANCE OF DESICCANT DEHUMIDIFIERS

**G. G. Ferreira, gabicp2@gmail.com**

**S. M. D. Santos, samuel.m.santos@eletrobras.com**

**L. A. Sphaier, lasphaier@id.uff.br**

Department of Mechanical Engineering / PGMEC, Universidade Federal Fluminense, Rua Passo da Pátria 156, bloco E, sala 216, Niterói, Rio de Janeiro, 24210-240, Brazil

**C. E. L. Nóbrega, nobrega@pobox.com**

Department of Mechanical Engineering, Centro Federal de Educação Tecnológica Celso Suckow da Fonseca, Rio de Janeiro, Brazil

**Abstract.** *This paper provides a comparison of two different methodologies for simulating the operation of desiccant wheels. One methodology is a correlation based on a system of two non-linear algebraic equations for determining the outlet states of the process (adsorption) and regeneration (desorption) streams, based on given inlet values and two performance parameters. However, in several literature studies, these parameters are given in terms of the quality of dehumidification provided ranging from high to low performance dehumidifiers. The other methodology, also seen in some literature studies is based on solving a PDE system that stems from heat and mass balances applied to the process streams and desiccant material in the wheel. Both methodologies are computationally implemented and simulation results are carried out for comparison purposes. The results, while still preliminary, provide an indication that for optimum thermal capacity ratios (which is directly related to the rotational speed), both formulations seem to agree; nevertheless, this is not seen for other situations.*

**Keywords:** *desiccant wheel, numerical simulation, cooling cycle, physical adsorption, evaporative cooling*

## 1. INTRODUCTION

Rotary dehumidifiers, commonly found in the form of active desiccant wheels, are used in the so-called desiccant cooling cycles, which employ air and water as the working fluids and require low-grade energy sources (Heidarinejad and Pasharshahi, 2011; Nóbrega and Brum, 2011; Panaras *et al.*, 2011; Nóbrega and Brum, 2012; Nóbrega and Sphaier, 2012, 2013; Sphaier and Nóbrega, 2012). These devices can be computationally simulated by means of detailed partial-differential equation (PDE) models (Sphaier and Worek, 2004, 2008, 2009; Simonson and Besant, 1997a,b). These mathematical models can range from detailed multi-dimensional transport equations to simple one-dimensional forms. Naturally, the increasing complexity of a model will require a greater amount of computational time. Regardless of the simplicity of one-dimensional PDE models, when performing the simulation of an entire thermodynamic cycle in which a desiccant wheel is employed, there is an even faster option. This alternative is based on using an algebraic correlation – commonly known as the non-linear analogy method (Maclaine-Cross and Banks, 1972; Banks, 1985a,b) – to simulate the behavior of the desiccant wheel. Although a may recent studies (Nóbrega and Brum, 2011; Panaras *et al.*, 2011; Nóbrega and Brum, 2012; Nóbrega and Sphaier, 2012, 2013; Sphaier and Nóbrega, 2012) have been using this cheaper option, there is an apparent lack of comparative studies. As a matter of fact it seems unclear from the literature to what extents of operating conditions could the simpler algebraic correlation be used. Under this scenario, the purpose of the current study is to provide a comparative analysis between the more detailed PDEs models and the classical algebraic correlation, in order to determine the range of application of the simpler approach. For completing this purpose, numerical simulations of a one-dimensional PDE model is carried out for different operating conditions and compared to the results obtained with the algebraic correlation.

## 2. PROBLEM FORMULATION

The general problem considered in this study is that of a rotary exchanger, which periodically alternates between different process streams. The rotary matrix is composed of numerous mini-channels through which the process streams flow, transferring mass and energy to the channel's walls, composed of a porous sorbent material. As mentioned, two types of models for predicting the operation of desiccant wheels will be compared, a PDE model, based on heat and mass energy balances, and a traditional non-linear algebraic correlation used by many investigations for wheel simulations within a complete cooling cycle.

### 2.1 PDE model

The simplifying assumptions for the PDE model used for the simulation of desiccant wheels are available in several sources, such as (Sphaier and Worek, 2004, 2008, 2009). With these assumptions, and considering a one-dimensional formulation for the process streams and sorbent materials the governing equations that result from simple mass and energy balances are given by:

The general problem considered in this study is that of a rotary exchanger, which periodically alternates between different process streams. The rotary matrix is composed of numerous mini-channels through which the streams flow, transferring mass and energy to the channel's walls, composed of a porous sorbent material. The simplifying assumptions for this problem are available in several sources, such as (Sphaier and Worek, 2004). With these assumption, and considering a one-dimensional formulation for the process streams and sorbent materials the governing equations that result from simple mass and energy balances are given by:

$$\rho_a \left( \frac{\partial Y}{\partial t} + (-1)^{\gamma_j} u_j \frac{\partial Y}{\partial x} \right) = \frac{\mathcal{P}_s}{\mathcal{A}_p} h_m \rho_a (Y_f - Y), \quad (1)$$

$$\rho c_p \left( \frac{\partial T}{\partial t} + (-1)^{\gamma_j} u_j \frac{\partial T}{\partial x} \right) = \frac{\mathcal{P}_s}{\mathcal{A}_p} h_m (T_f - T) + \frac{\mathcal{P}_s}{\mathcal{A}_p} h_m \rho_a \varphi c_{p,v} (Y_f - Y) (T_f - T). \quad (2)$$

$$\epsilon \rho_a \frac{\partial Y_f}{\partial t} + (1 - \epsilon) \rho_s f_s \frac{\partial W}{\partial t} = - \frac{\mathcal{P}_s}{\mathcal{A}_f} h_m \rho_a (Y_f - Y) \quad (3)$$

$$\rho_f c_f \frac{\partial T_f}{\partial t} = - \frac{\mathcal{P}_s}{\mathcal{A}_f} h_m (T_f - T) + \frac{\mathcal{P}_s}{\mathcal{A}_f} h_m \rho_a (1 - \varphi) c_{p,v} (Y_f - Y) (T_f - T) + (1 - \epsilon) \rho_s f_s \frac{\partial W}{\partial t} i_{sor}, \quad (4)$$

These equations are valid for a general period  $j$ , in which the time variable varies from  $t_{0,j}$  to  $t_{0,j} + t_j$ .

The  $\varphi$  parameter determines which medium is directly affected by the sensible heating term. If  $\varphi = 1$  the sensible heating is entirely delivered to the process stream; on the other hand, if  $\varphi = 0$  it is entirely delivered to the sorbent felt. Any other value will lead to a fraction of this effect being delivered to each of these media. A similar consideration is done in (Simonson and Besant, 1997a, 1999); however, it is also considered that the latent fraction of the sorption heating effect can be delivered partly to the felt and partly to the process stream.

In dimensionless form, the governing equations are given by:

$$\tau_j \frac{\partial Y^*}{\partial t^*} + (-1)^{\gamma_j} \frac{\partial Y^*}{\partial x^*} = N_{tu,j}^m (Y_f^* - Y^*), \quad (5)$$

$$\chi \left( \tau_j \frac{\partial T^*}{\partial t^*} + (-1)^{\gamma_j} \frac{\partial T^*}{\partial x^*} \right) = N_{tu,j}^h (T_f^* - T^*) + \varphi N_{tu,j}^m c_p^* (Y_f^* - Y^*) (T_f^* - T^*), \quad (6)$$

$$\epsilon \frac{\partial Y_f^*}{\partial t^*} + (1 - \epsilon) \Omega \frac{\partial W^*}{\partial t^*} = - \frac{N_{tu,j}^m}{V_{r,j}^*} (Y_f^* - Y^*) \quad (7)$$

$$\chi_f \frac{\partial T_f^*}{\partial t^*} = - \frac{N_{tu,j}^h}{C_{r,j}^*} (T_f^* - T^*) + (1 - \varphi) \frac{N_{tu,j}^m}{C_{r,j}^*} c_p^* (Y_f^* - Y^*) (T_f^* - T^*) + (1 - \epsilon) \Omega \frac{\partial W^*}{\partial t^*} \chi_{sor} i_{vap,ref}^* \quad (8)$$

where the dimensionless variables are given by:

$$x^* = \frac{x}{L}, \quad dt^* = \frac{dt}{t_j}, \quad T^* = \frac{T - T_{\min}}{T_{\max} - T_{\min}}, \quad Y^* = \frac{Y}{Y_{\max}}, \quad W^* = \frac{W}{W_{\max}}, \quad (9)$$

and the dimensionless parameters are defined as:

$$\Omega = \frac{\rho_s f_s W_{\max}}{\rho_a Y_{\max}}, \quad N_{tu,j}^m = \frac{h_m P_s L}{u_j A_p}, \quad N_{tu,j}^h = \frac{h_h P_s L}{\rho_a c_{p,a} u_j A_p}, \quad c_p^* = \frac{c_{p,v} Y_{\max}}{c_{p,a}}, \quad (10)$$

$$\tau_j = \frac{L}{u_j t_j}, \quad V_{r,j}^* = \frac{L A_f}{A_p u_j t_j} = \frac{A_f}{A_p} \tau_j, \quad C_{r,j}^* = \frac{\rho_b c_s}{\rho_a c_{p,a}} V_{r,j}^*, \quad i_{vap,ref}^* = \frac{\rho_a Y_{\max} i_{vap,ref}}{\Delta T \rho_b c_s} \quad (11)$$

where  $\rho_b = (1 - \epsilon) \rho_s$ .

The coefficients  $\chi$  and  $\chi_f$  take into account variations in heat capacity due to the presence of moisture, in the airstream, and in the sorbent material, respectively. These are given by:

$$\chi = \frac{\rho c_p}{\rho_a c_{p,a}} = 1 + \frac{c_{p,v}}{c_{p,a}} Y, \quad \chi_{sor} = \frac{i_{sor}}{i_{vap,ref}} \quad (12)$$

$$\chi_f = \frac{c_f \rho_f}{c_s \rho_b} = \frac{1}{c_s \rho_b} \left( \epsilon \rho_a (c_{p,a} + c_{p,v} Y_f) + (1 - \epsilon) \rho_{fs} \left( c_s + f_s \left( W c_{ls} + \left( \frac{\partial \Delta i_{wet}}{\partial T_f} \right)_W \right) \right) \right) \quad (13)$$

The heat of sorption and the heat of wetting (in differential and integral forms) are commonly expressed in terms of the heat of vaporization:

$$i_{sor} = (1 + e_{sor}) i_{vap}, \quad i_{wet} = -e_{sor} i_{vap}, \quad \text{with} \quad i_{vap} = i_{vap,ref} + (c_{p,v} - c_{ls})(T - T_{ref}) \quad (14)$$

$$\Delta i_{wet} = \int_0^W i_{wet} dW' = -i_{vap} \bar{e}_{sor} W, \quad \text{where} \quad \bar{e}_{sor}(W) = \frac{1}{W} \int_0^W e_{sor} dW \quad (15)$$

$$\chi_{sor} = (1 + e_{sor}) \left( 1 + \frac{(c_{p,v} - c_{ls})(T - T_{ref})}{i_{vap,ref}} \right) \quad (16)$$

In terms of the dimensionless variables the coefficient  $\chi$  and  $\chi_f$  are reduced to:

$$\chi = 1 + c_p^* Y^*, \quad \chi_f = \epsilon \frac{V_r^*}{C_r^*} (1 + c_p^* Y_f^*) + 1 + c_{ls}^* W^* - (c_{ls}^* - c_v^*) \bar{e}_{sor} W^*, \quad (17)$$

where  $c_{ls}^*$  and  $c_v^*$ , are additional dimensionless parameters given by:

$$c_{ls}^* = \frac{f_s W_{\max} c_{ls}}{c_s}, \quad c_v^* = \frac{f_s W_{\max} c_{p,v}}{c_s} = c_p^* \frac{V_r^*}{C_r^*} \Omega (1 - \epsilon), \quad (18)$$

An expression for  $e_{sor}$ , and consequently  $\bar{e}_{sor}$ , can be obtained from study (San, 1993) for silica-gel and water:

$$e_{sor} = a \exp(-b W^*), \quad W^* \bar{e}_{sor} = \frac{a}{b} (1 - \exp(-b W^*)) \quad (19)$$

where  $a = 0.2843$  and  $b = 10.28 W_{\max}$ , where  $W_{\max}$  is the maximum water uptake in the desiccant.

A commonly used and simple isotherm is the separation-factor based relation:

$$W = \frac{\phi_f W_{\max}}{r + (1 - r) \phi_f}, \quad (20)$$

where  $r$  is the separation factor and  $\phi_f$  is the relative humidity of air in the pore space, i.e.  $\phi_f = \phi_f(T_f, Y_f)$ . For  $r = 1$ , the isotherm is simplified to the so-called liner-type, which will be used for calculating the results presented in this work.

### 2.1.1 Boundary and periodicity conditions

For the process stream, the presence of first order spatial derivatives only require a single boundary condition for each dependent variable. These are the inlet conditions of the two process streams. A counterflow arrangement is considered which leads to the following conditions:

$$Y^*(0, t) = Y_{in}^* \quad \text{and} \quad T^*(0, t) = 0, \quad \text{for adsorption period} \quad (21)$$

$$Y^*(1, t) = Y_{in}^* \quad \text{and} \quad T^*(1, t) = 1, \quad \text{for regeneration period} \quad (22)$$

These boundary conditions are applied repetitively, starting from an equilibrium condition, until a periodic regime is attained. The value of the dimensionless concentration of both inlets is calculated considering an ambient condition of 50% relative humidity and 25°C (considered as the minimum reference temperature). The value for the maximum temperature corresponds to the regeneration temperature, which in this work will be considered as 70°C (typical for silica-gel coated wheels).

### 2.1.2 Performance assessment

The dehumidification performance is usually assessed by calculating the dehumidification efficiency, defined as:

$$\eta_{dw} = \frac{Y_{ads,in} - \bar{Y}_{ads,out}}{Y_{ads,in} - Y_{ads,out,ideal}}, \quad (23)$$

where the over-bar denotes an outlet averaged value, which is calculated to account for the outlet air humidity (as well as other properties) variation with the angular position of the wheel. This average can be easily translated into the dimensionless time variable, such that:

$$\bar{Y}_{ads,out} = \int_0^1 Y_{ads,out} dt^* \quad (24)$$

### 2.1.3 Notation simplification

In order to simplify the notation, the dimensional outlets of each process stream are described by numbers, such that:

$$Y_1^* = Y_{ads,in}^*, \quad T_1^* = T_{ads,in}^*, \quad (25a)$$

$$Y_2^* = \bar{T}_{ads,out}^*, \quad T_2^* = \bar{T}_{ads,out}^*, \quad (25b)$$

$$Y_3^* = Y_{reg,in}^*, \quad T_3^* = T_{reg,in}^*, \quad (25c)$$

$$Y_4^* = \bar{T}_{reg,out}^*, \quad T_4^* = \bar{T}_{reg,out}^*. \quad (25d)$$

## 2.2 Algebraic formulation

An alternative, and much faster option for simulating desiccant wheels, is to use an algebraic correlation for determining the outlet states in terms of the inlet data. One such methodology stems from the analogy method developed by (Maclaine-Cross and Banks, 1972; Banks, 1985a,b), which is base on the following equations for potentials  $\eta$ :

$$\eta_1 = (F_1(T_2, Y_2) - F_1(T_1, Y_1)) / (F_1(T_3, Y_3) - F_1(T_1, Y_1)), \quad (26)$$

$$\eta_2 = (F_2(T_2, Y_2) - F_2(T_1, Y_1)) / (F_2(T_3, Y_3) - F_2(T_1, Y_1)), \quad (27)$$

where the involved temperatures and humidity ratios have been described in equations (25). The coefficients  $\eta_1$  and  $\eta_2$  depend on the type of desiccant wheel and the functions  $F_1$  and  $F_2$  are defined in terms of temperature and absolute

humidity as:

$$F_1(T, Y) = -\frac{2865}{(T + 273.15)^{1.49}} + 4.344Y^{0.8624}, \quad (28)$$

$$F_2(T, Y) = \frac{(T + 273.15)^{1.49}}{6360} - 1.127Y^{0.07969} \quad (29)$$

These equations, together with global heat and mass balances across the desiccant wheel, allow the determination of the outlet states once the inlet states are known. Typical values for  $\eta_1$  and  $\eta_2$  are given in Table 1: In the present analysis,

Table 1. Typical Values for  $\eta_1$  and  $\eta_2$ .

Wheel Type	$\eta_1$	$\eta_2$
Good Performance (GP)	0.08	0.8
Moderate Performance (MP)	0.076	0.85
Poor Performance (PP)	0.10	0.7

the values for a good performance wheel (GP) and a poor performance wheel (PP) will be analysed as limiting cases.

### 3. RESULTS AND DISCUSSION

The partial differential model given by equations (26) is solved using a finite-volumes scheme combined with the numerical method of lines, as described in (Sphaier and Worek, 2008), which was implemented in the Wolfram Mathematica platform. Table 2 lists the values adopted for the dimensionless and dimensional parameters used in the solution of the PDE model.

Table 2. Values for parameters in PDE model.

Number of heat transfer units, $N_{tu,j}^h$	100
Number of mass transfer units, $N_{tu,j}^m$	100
Fraction of sensible heat to stream, $\varphi$	0
Area ratio, $A_f/A_p$	0.1
Felt porosity, $\epsilon$	0.3

The main problem in comparing the algebraic correlation with the PDE model is there are many unknowns that lead to the correlation. Because of this two limiting cases of the correlation parameters were chosen, as mentioned previously and for the dimensionless parameters that are needed as input in the PDE model solution the following strategy was used:

1. Since it is know that increasing the number of transfer units for heat and mass transfer generally leads to asymptotically increasing dehumidification efficiency, values large enough to ensure that re results are independent of the NTUs were chosen;
2. Material properties related to silica-gel, a common desiccant were adopted;
3. Balanced and symmetric wheels are considered, such that parameters that could assume different values for each period are equal;
4. Since the operation period, and parameters that depend on it, can have a big influence on the wheel performance characteristics, values that are close to the optimum value are analyzed.

Regarding the last point, the optimization is carried-out based on the value of  $C_{r,j}^*$ , and the other time-dependent parameters ( $V_{r,j}^*$  and  $\tau_j$ ) are varied proportionally. With this in mind, the first results, displayed in figure 1, present the variation of the dehumidification efficiency calculated for different  $C_{r,j}^*$  values, and different regeneration temperatures. As can be seen from these results, the dehumidification efficiency reaches a maximum for smaller values of the heat

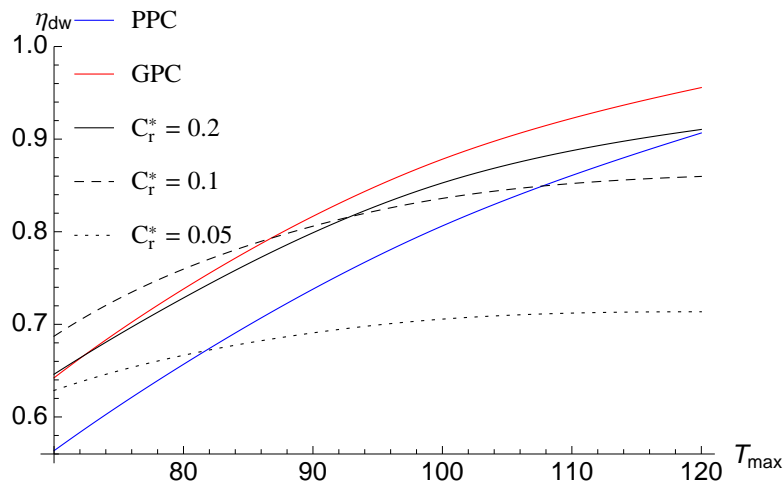


Figure 1. Variation of dehumidification efficiency with heat capacity ratio for different regeneration temperatures.

capacity ratio  $C_{r,j}^*$ , and from there on decrease almost linearly. These maximum values are obtained for  $C_{r,j}^* = 0.10$  for  $T_{\max} = 75$  and  $C_{r,j}^* = 0.17$  for  $T_{\max} = 120$ . Based on this initial analysis, the subsequent comparisons will consider 0.1, 0.2 and 0.05 as the values of  $C_{r,j}^*$ .

The next results present a comparative analysis of the outlet temperatures and humidity ratios for the process (adsorption) stream,  $T_2^*$  and  $Y_2^*$ , and the regeneration stream,  $T_4^*$  and  $Y_4^*$ , as well as the dehumidification efficiency. The analysis is performed by varying the regeneration temperature, while keeping the remaining parameters fixed, for the PDE model solution calculated with the three values of  $C_{r,j}^*$  mentioned previously, and comparing the results with those obtained with the algebraic correlation, calculated for the two limiting cases of a good performance wheel (GP) and poor performance wheel (PP). Figure 2 presents the variation of the dehumidification efficiency with the regeneration temperature for the previously mentioned cases. As one can observe, for  $C_{r,j}^* = 0.2$ , the dehumidification efficiency calculated with the PDE

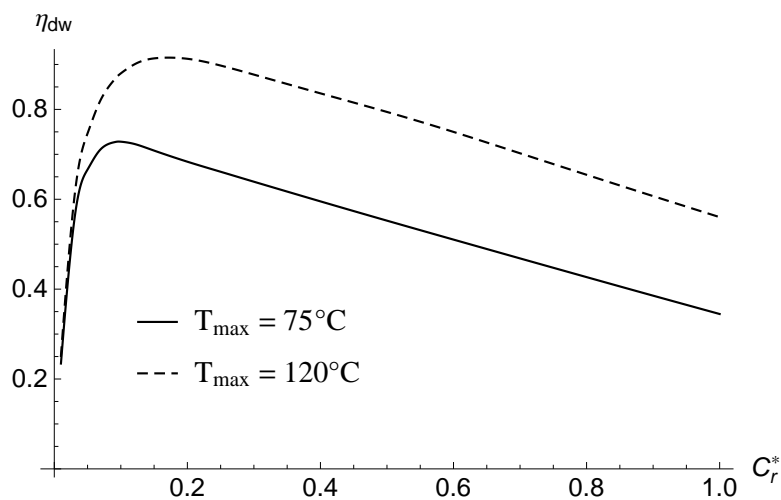


Figure 2. Variation of dehumidification efficiency with regeneration temperature calculated with the algebraic correlation (PPC and GPC) and the PDE model (for different  $C_{r,j}^*$  values).

model yields values that stay within the two limiting cases calculated with the algebraic calculation. When looking into the PDE solutions for the other heat capacity ratio cases, one notices that the case with  $C_{r,j}^* = 0.1$  gives higher dehumidification efficiencies for lower regeneration temperatures, as foreseen by the analysis presented in figure 1. As a matter of fact, the dehumidification efficiencies values are higher than those predicted by the algebraic correlation for the good performance wheel. Next, figure 3 presents similar comparative results for the outlet temperature of the process stream.

As can be seen, different than what was observed for the dehumidification efficiency, the outlet temperatures predicted

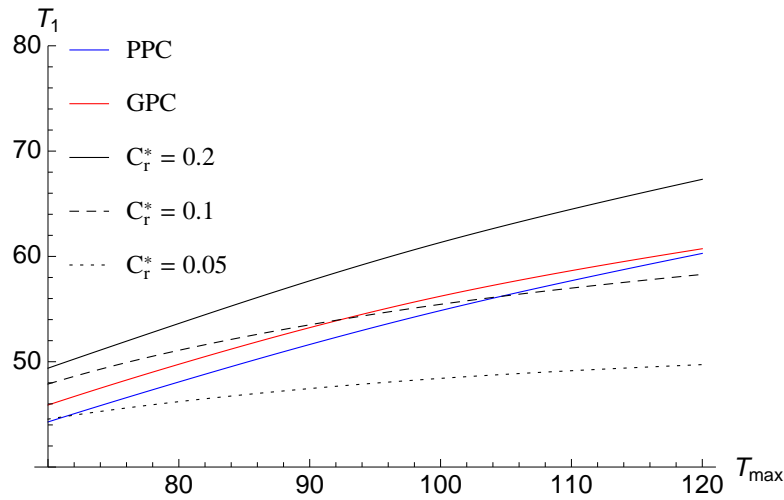


Figure 3. Variation of process side outlet temperature with regeneration temperature calculated with the algebraic correlation (PPC and GPC) and the PDE model (for different  $C_{r,j}^*$  values).

by the correlation are very similar for both limiting cases (poor performance wheel and good performance wheel). On the other hand, the results calculated for the different capacity ratios with the PDE model span over a wider range. This could be an indication of a problem with the algebraic correlation in correctly predicting the outlet temperatures. The next figure, presents the results of the outlet humidity ratios of the process stream. As expected, since this outlet value is directly related to the dehumidification efficiency, the results have the same tendency seen in figure 2.

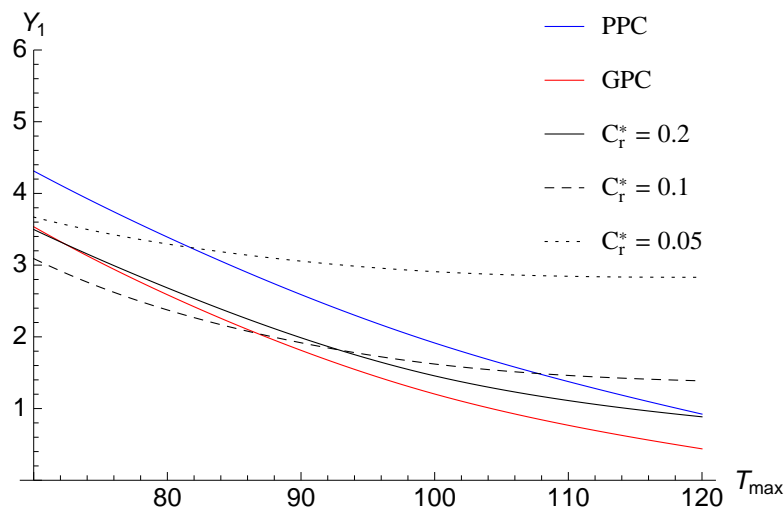


Figure 4. Variation of process side outlet humidity ratio with regeneration temperature calculated with the algebraic correlation (PPC and GPC) and the PDE model (for different  $C_{r,j}^*$  values).

The two final figures (figs. 5 and 6) present the outlet values (temperature and humidity ratio) of the regeneration stream calculated with the different methodologies for different regeneration temperatures. As one can infer from the presented results, the outlet humidity for almost all cases have the same tendency, and yield small variations. When looking into the outlet temperature results (fig. 5), one notices, again, that the results calculated with the correlation for the two limiting cases are very close to each other, and that the PDE solution case that approached better these cases is the case with  $C_{r,j}^* = 0.1$ .

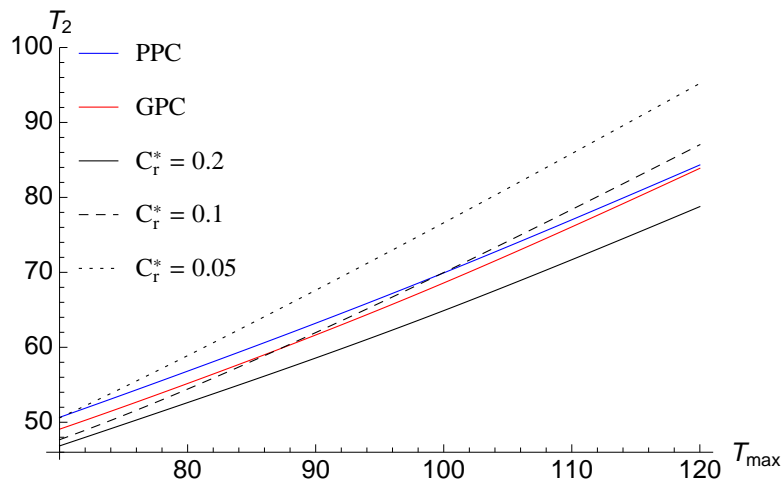


Figure 5. Variation of regeneration side outlet temperature with regeneration temperature calculated with the algebraic correlation (PPC and GPC) and the PDE model (for different  $C_{r,j}^*$  values).

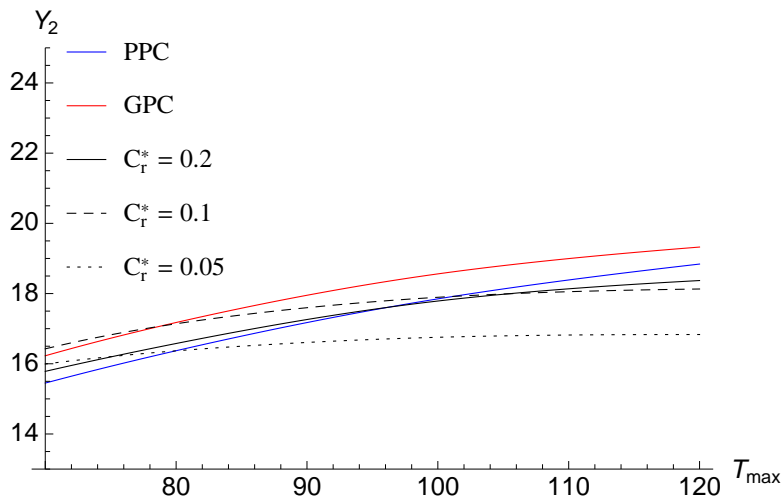


Figure 6. Variation of regeneration side outlet humidity ratio with regeneration temperature calculated with the algebraic correlation (PPC and GPC) and the PDE model (for different  $C_{r,j}^*$  values).

#### 4. CONCLUSIONS

This paper presented a comparison between two different methodologies for predicting the operational of desiccant wheels. A traditionally adopted methodology, based on an algebraic correlation developed in the 70-80s, and a partial differential equations model, based on mass and energy balances for the desiccant material and adjacent channels. The comparison of such models is not straightforward since there are many parameters that can influence the results calculated with the PDE model, whereas the widely algebraic correlation has little room for modifications. Nevertheless, some hypotheses were done in order to eliminate the influence of some parameters, by choosing common desiccant material properties, and using large number of transfer units. With these considerations, an initial comparison of the two models was carried out, and the results showed that for heat capacity ratios (which depend directly on the wheel rotational speed) that approach the optimum values, the PDE model results and the algebraic correlation model present a reasonable agreement; however, when away from the optimum values, the results present a divergent behavior. When comparing the outlet values for both streams calculated with the two different methodologies, one notices a greater discrepancy for the outlet temperatures than for the outlet humidities. While these are still the first comparative results calculated so far, one could begin to suspect that the algebraic correlation could be well suited for predicting humidity values, while providing

incorrect values for the outlet temperatures.

## 5. ACKNOWLEDGEMENTS

The authors would like to acknowledge the financial support received by FAPERJ, CNPq and CAPES.

## REFERENCES

- Banks, P.J., 1985a. "Prediction of heat and mass regenerator performance using nonlinear analogy method: Part I – Basis". *Journal of Heat Transfer (ASME)*, Vol. 107, pp. 222–229.
- Banks, P.J., 1985b. "Prediction of heat and mass regenerator performance using nonlinear analogy method: Part II – Comparison of methods". *Journal of Heat Transfer (ASME)*, Vol. 107, pp. 230–238.
- Heidarinejad, G. and Pasharshahi, H., 2011. "Potential of a desiccant-evaporative cooling-system performance in a multi-climate country". *International Journal of Refrigeration*, Vol. 34, No. 5, pp. 1251–1261.
- Maclaine-Cross, I.L. and Banks, P.J., 1972. "Coupled heat and mass transfer in regenerators – Predictions using an analogy with heat transfer". *International Journal of Heat and Mass Transfer*, Vol. 15, No. 6, pp. 1225–1242.
- Nóbrega, C.E.L. and Brum, N.C.L., 2011. "A graphical procedure for desiccant cooling cycle design". *Energy*, Vol. 36, No. 3, pp. 1564–1570.
- Nóbrega, C.E.L. and Brum, N.C.L., 2012. "An analysis of the heat and mass transfer roles in air dehumidification by solid desiccants". *Energy and Buildings*, Vol. 50, pp. 251–258.
- Nóbrega, C.E.L. and Sphaier, L.A., 2012. "Modeling and simulation of a Desiccant-Brayton cascade refrigeration cycle". *Energy and Buildings*, Vol. 55, pp. 575–584.
- Nóbrega, C.E.L. and Sphaier, L.A., 2013. "Desiccant-assisted humidity control for air refrigeration cycles". *International Journal of Refrigeration*, Vol. 36, No. 4, pp. 1183–1190.
- Panaras, G., Mathioulakis, E. and Belessiotis, V., 2011. "Solid desiccant air-conditioning systems-design parameters". *Energy*, Vol. 36, No. 5, pp. 2399–2406.
- San, J., 1993. "Heat and mass transfer in a two-dimensional cross-flow regenerator with a solid conduction effect". *International journal of heat and mass transfer*, Vol. 36, No. 3, pp. 633–643.
- Simonson, C.J. and Besant, R.W., 1997a. "Heat and moisture transfer in desiccant coated rotary energy exchangers: Part I. numerical model". *HVAC&R Research*, Vol. 3, No. 4, pp. 325–350.
- Simonson, C.J. and Besant, R.W., 1997b. "Heat and moisture transfer in desiccant coated rotary energy exchangers: Part II. validation and sensitivity studies". *HVAC&R Research*, Vol. 3, No. 4, pp. 351–368.
- Simonson, C.J. and Besant, R.W., 1999. "Energy wheel effectiveness – part I: Development of dimensionless groups". *International Journal of Heat and Mass Transfer*, Vol. 42, pp. 2161–2170.
- Sphaier, L.A. and Nóbrega, C.E.L., 2012. "Parametric analysis of components effectiveness on desiccant cooling system performance". *Energy*, Vol. 38, No. 1, pp. 157–166.
- Sphaier, L.A. and Worek, W.M., 2004. "Analysis of heat and mass transfer in porous sorbents used in rotary regenerators". *International Journal of Heat and Mass Transfer*, Vol. 47, No. 14-16, pp. 3415–3430.
- Sphaier, L.A. and Worek, W.M., 2008. "Numerical solution of periodic heat and mass transfer with adsorption in regenerators: Analysis and optimization". *Numerical Heat Transfer, Part A: Applications*, Vol. 53, No. 11, pp. 1133–1155.
- Sphaier, L.A. and Worek, W.M., 2009. "Parametric analysis of heat and mass transfer regenerators using a generalized effectiveness-NTU method". *International Journal of Heat and Mass Transfer*, Vol. 52, No. 9–10, pp. 2265–2272.